Global ocean heat content 1955–2008 in light of recently revealed instrumentation problems

Article · April 2009

DOI: 10.1029/2008GL037155

Hernan Garcia
National Oceanic and Atmospheric Administrat…

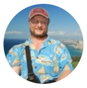

Alexey V Mishonov
National Oceanic and Atmospheric Administrat…

GEOPHYSICAL RESEARCH LETTERS, VOL. 36, L07608, doi:10.1029/2008GL037155, 2009

Global ocean heat content 1955–2008 in light of recently revealed instrumentation problems

S. Levitus,[1] J. I. Antonov,[1] T. P. Boyer,[1] R. A. Locarnini,[1] H. E. Garcia,[1] and A. V. Mishonov[1]

Received 31 December 2008; revised 26 February 2009; accepted 18 March 2009; published 11 April 2009.

[1] We provide estimates of the warming of the world ocean for 1955–2008 based on historical data not previously available, additional modern data, correcting for instrumental biases of bathythermograph data, and correcting or excluding some Argo float data. The strong interdecadal variability of global ocean heat content reported previously by us is reduced in magnitude but the linear trend in ocean heat content remain similar to our earlier estimate. **Citation:** Levitus, S., J. I. Antonov, T. P. Boyer, R. A. Locarnini, H. E. Garcia, and A. V. Mishonov (2009), Global ocean heat content 1955–2008 in light of recently revealed instrumentation problems, *Geophys. Res. Lett.*, *36*, L07608, doi:10.1029/2008GL037155.

1. Introduction

[2] We have previously reported estimates of the variability of the ocean heat content (OHC) of the world ocean [*Levitus et al.*, 2000, 2005a]. The warming trend in OHC dominated earth's heat balance during the past fifty years [*Levitus et al.*, 2001] and the trend has been attributed to the increase in greenhouse gases in earth's atmosphere by *Levitus et al.* [2001] and *Barnett et al.* [2001, 2005] among others.

[3] Here we update these estimates for the upper 700 m of the world ocean (OHC700) with additional historical and modern data [*Levitus et al.*, 2005b; *Boyer et al.*, 2006] including Argo profiling float data that have been corrected for systematic errors. We apply empirically determined corrections for instrumental offsets of bathythermograph (BT) measurements (both expendable bathythermographs (XBT) and mechanical bathythermographs (MBT)) using near-contemporaneous data from Ocean Station Data casts (OSD) (reversing thermometers) and Conductivity-Temperature-Depth (CTD) casts similar in technique to *Gouretski and Koltermann* [2007] (hereinafter referred to as GK07). The purpose of this paper is to determine the effect of correcting for these BT biases on our estimates of OHC700. The source of the time-varying bias in MBT measurements is unknown. We make a correction for this bias here and will investigate the source of this bias in future work. We acknowledge that ocean temperature data are sparse in the polar and subpolar regions of the world ocean but we still refer to our OHC estimates as global. We do this because the OHC estimates are volume integrals so that only relatively small contributions are expected from the polar regions to our global estimates. Nevertheless there are locally important changes in OHC in these regions such as warming of the North Atlantic Water in the Arctic Ocean that may play an important role in climate change.

[4] XBT instruments do not directly measure the depth of each temperature observation as they fall through the water column after entering the sea surface. Instead depth of observation is computed using a fall-rate equation and the time elapsed since the XBT entered the water. An international meeting was held during March 2008 at the NOAA Atlantic Oceanographic and Meteorological Laboratory in Miami to discuss the XBT fall-rate problem. One of the results of the meeting was to establish a web page that contains known references to the XBT bias problem including fall-rate inaccuracies and a collection of data gathered simultaneously by XBT and OSD/CTD instruments which can be used to study the fall-rate problem. This page has been established at www.nodc.noaa.gov.

[5] *Wijffels et al.* [2008] (hereinafter referred to as W08) and *Ishii and Kimoto* [2009] (hereinafter referred to as IK09) have associated the XBT biases with a change in the fall-rate of XBT instruments as a function of the year of manufacture. They also note that constant temperature offsets have been found in some CTD/XBT comparisons studies (see www.nodc.noaa.gov). Here we show that the time-varying XBT bias appears to be due to both of these types of errors. Our method of correcting for the XBT time-varying bias reflects this finding. Our results show that even after applying recently developed time-varying fall-rate corrections (W08, IK09) there are still substantial temperature differences between near-contemporaneous XBT and OSD/CTD profiles in the upper 100 m of the ocean.

[6] We emphasize that our work represents an attempt to correct for observed XBT biases and that more work remains to solve this problem. Complicating any attempt to correct XBT biases, whatever their origin, is the fact that many historical XBT profiles archived at NODC and contained in *World Ocean Database 2005* (WOD05) do not contain metadata indicating model type. These metadata deficiencies influenced how we have attempted to compute a correction for the XBT bias error.

[7] GK07 claim that there is a positive systematic bias in XBT data on average of 0.2–0.4°C that leads to overestimates of OHC increase during the past 50 years. They further claim that in the upper 200 m of the world ocean after 1995 the XBT "warm bias" exceeds 0.5°C. Our results confirm that there are offsets for both XBT and MBT temperature data compared to contemporary data from bottles and CTD instruments but that the magnitude of these offsets is not as great as claimed by GK07. Also, we find that their claim that using bias-corrected XBT data reduces our earlier estimates of OHC change since the 1950s by a factor of 0.6 is not correct. Figure 1 shows our earlier result

[1]National Oceanographic Data Center, NOAA, Silver Spring, Maryland, USA.

0094-8276/09/2008GL037155$05.00

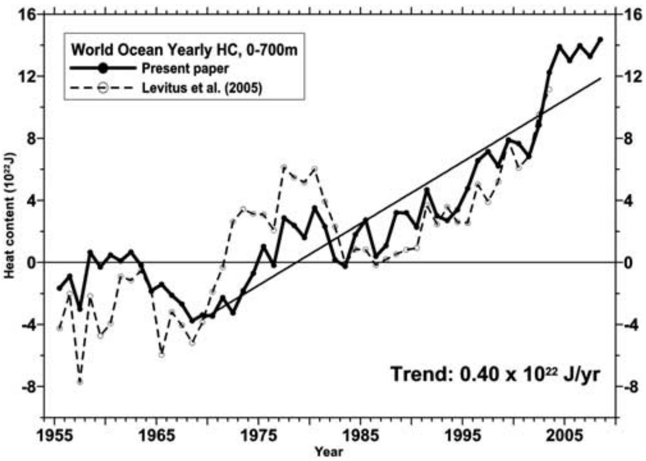

Figure 1. Time series of yearly ocean heat content (10^{22}J) for the 0–700 m layer from this study (solid) and from *Levitus et al.* [2005a] (dashed). Each yearly estimate is plotted at the midpoint of the year. Reference period is 1957–1990.

[*Levitus et al.*, 2005a] and our present result with additional data and corrections applied as described in this article. Interdecadal variability is reduced but the long-term trends for the two analyses for the 1955–2003 period are similar. After 2003, OHC700 increases to a plateau during 2004–2008. Table S1 of the auxiliary material provides statistics of OHC700 for the world ocean and individual basins for the 1969–2008 period.[1] The starting year is chosen because data coverage improved after the mid 1960s when XBT measurements of the upper ocean began. The linear trends (with 95% confidence intervals) of OHC700 are $0.40 \times 10^{22} \pm 0.05$ J yr^{-1} for 1969–2008 and is $0.27 \times 10^{22} \pm 0.04$ J yr^{-1} for 1955–2008. These statistics are based on the yearly mean heat content values determined as the average of the four seasons (see section 5). Heat storage in Table S1 is per unit area of ocean surface.

2. Data and Method

[8] To identify possible offsets in temperature measurements from MBT and XBT data we initially followed the method of GK07. We converted synoptic temperature profiles to anomaly profiles by subtracting out the climatological monthly mean temperature value at each standard depth level in the vertical using our objectively analyzed fields of temperature. This reduces the influence of the annual cycle. Note that these climatologies initially included the biased XBT and MBT data. Next we averaged all XBT anomaly observations on a $2° \times 4° \times$ 1-year grid at the sixteen standard depth levels used in *World Ocean Atlas 2005* [*Locarnini et al.*, 2006] in the upper 700 m of the world ocean. We do the same separately for MBT data (eleven standard levels in the upper 250 m of the world ocean; there are approximately 2.3 million MBT profiles in WOD05 of which approximately 480,000 reach 250 m depth). We also performed this averaging separately for the combination of temperature measurements from OSD and CTD casts. At each standard level for each year we computed the differences between XBT and OSD/CTD averages for each $2° \times 4°$ gridbox and do the same for MBT and OSD/CTD averages. For each standard level and year we computed the median of the differences of all gridboxes. Using the median as opposed to the arithmetic average is critical because it reduces the influence of outliers on the estimates of the differences between the BT data and the OSD/CTD data. To illustrate the importance of using the median, Figure S1 shows the frequency distribution of global XBT minus OSD/CTD differences for $2° \times 4°$ gridboxes for the year 1999 at 150 m depth. The median of the differences shown is 0.079°C and the arithmetic mean is 0.163°C. Examination of other frequency distributions of this type by year and depth indicate the presence of numerous outliers and non-normality of frequency distributions. Thus medians are preferred for computing the average differences between these data types. Figure S2 shows time series of the number of MBT minus OSD/CTD difference pairs and the number of XBT minus OSD/CTD difference pairs. Note the large decrease in MBT-(OSD/CTD) data pairs after 1986 and a large decrease in XBT-(OSD/CTD) data pairs after 1994. Figure S3 shows that most XBT-OSD/CTD difference pairs occur in the mid-latitudes of the northern hemisphere. The same is true for MBT difference pairs.

[9] Figure S4a is a plot of the differences between XBT and OSD/CTD data as a function of year and depth from GK07 based on the arithmetic mean. Figure S4b is our estimate based on using medians as opposed to arithmetic means. Figure S5a is a plot of the differences between MBT and OSD/CTD data as a function of year and depth from GK07 and Figure S5b is our corresponding plot based on medians as opposed to arithmetic means. In both comparisons, estimates of the differences between instrument types using medians as opposed to arithmetic means tend to be smoother as a function of time and smaller in magnitude. In Figures S4 and S5 at least thirty $2° \times 4°$ grid boxes for each year and standard depth level must exist for the data point to be plotted. We further smoothed our difference fields by computing 5-year running means. We applied these corrections to the XBT and MBT standard depth temperature values and recomputed the monthly climatologies used to remove the annual cycle and then repeated the entire procedure a second time to minimize the biases. This iteration is necessary because the monthly climatologies we use to compute anomalies include the biased XBT and MBT data. Figures 2 and S6 respectively show the corrections that we have applied to the XBT and MBT profiles after the two iterations. Figures S7 and S8 show that the global average biases in the XBT and MBT values at each depth are reduced to near zero.

[10] The results of GK07 and our work show that for both (XBT)-(OSD/CTD) differences and (MBT)-(OSD/CTD) differences that a subsurface maximum (50–100 m) occurs. This can be due to sampling the shallow tropical permanent thermocline but is most likely due to sampling seasonal thermoclines in the extratropics since the extratropics is where most of our difference pairs occur and our database has more measurements from warmer as opposed to colder seasons. Differences between response times of thermistors

[1] Auxiliary materials are available in the HTML. doi:10.1029/2008GL037155.

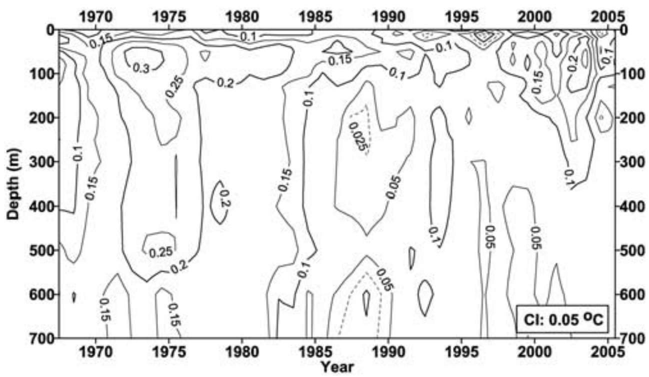

Figure 2. Time series (5-year running means) of the temperature corrections based on medians of the differences (°C) applied to XBT observations. Calculations are based on at least 30 overlapping $2° \times 4°$ boxes per year and level.

in BTs as well as differences in response time of the pressure measuring sensor in MBTs and inaccurate fall-rate equation in XBTs could each play some role in the existence of a subsurface maximum in these difference statistics.

[11] We eliminated the effect of BT offsets by subtracting the global average differences shown in Figures 2 and S6 from each XBT and MBT profile respectively at each standard depth level for each year in which the BT profile was measured. Using all corrected data we recomputed monthly climatologies of temperature at standard depth levels. We then computed all-data yearly and seasonal temperature anomaly fields by subtracting the corresponding climatological one-degree square monthly mean temperature value from each standard level temperature value in each temperature profile. The final step was to compute yearly OHC700 fields.

[12] There is one difference in data processing between our earlier works and our present work. Previously we computed climatological monthly means by averaging all data in each 1°-square for each climatological month regardless of year of observation. Now we compute decadal monthly means by averaging all data within each month for decadal periods beginning with 1955–1964 and then averaging these decadal climatological monthly means to compute the long-term climatological monthly mean (1955–2006). This is necessary because of the large amount of Argo profiling float data introduced to the observing system in recent years which can bias climatologies to the Argo sampling period. The last "decade" for compositing was actually 1995–2006.

3. Comparison With Other Estimates

[13] Figure S9 compares our present result with estimates by *Domingues et al.* [2008] (hereinafter referred to as D08) and IK09. All three estimates of OHC700 exhibit a similar linear trend but there are differences in the year-to-year variability. These estimates all use different processing methods and there are some differences in the data used. For example D08 do not use any MBT data in their study. We compare the linear trends for the 1969–2003 period since 1969 is a few years after XBTs began to be used in large numbers and 2003 is the last common year of analysis for the three estimates. For our results, the IK09 results, and the D08 results the trends (with 95% confidence intervals) are 0.32 ± 0.05, 0.24 ± 0.04, and $0.41 \pm 0.06 \times 10^{22}$ J yr^{-1} respectively. The general agreement of the three results suggests that the global linear trend is qualitatively robust to processing methods although there are differences in the magnitude of the trend. However there is reason to question the D08 results as we shall show.

[14] To further investigate the effect of the different methods of determining corrections to the XBT bias problem we have separately applied the XBT fall-rate corrections developed by W08 [*Wijffels et al.*, 2008, Table 1] and IK09 to the database used to compute our OHC700 estimate in this paper. Figure S10 shows time series of OHC700 based on the W08 corrections and the D08 estimate. After the mid 1990s substantial differences between the W08-based series and the D08 series occur with the W08-based series decreasing in magnitude before substantially increasing after 2001. We do find good agreement between IK09 and our computation of OHC700 using the IK09 corrections applied to our database (not shown).

[15] It is revealing to examine the differences between XBT data corrected using W08 and the OSD/CTD data in $4° \times 2° \times$ 1-year (based on 5-year running mean) boxes as we did in Figure 2. Figure 3 shows the results of this computation. A clear subsurface maxima appears at approximately 50 m depth as a function of year indicating a systematic time-varying global average XBT temperature bias that has not been eliminated by the time-varying fall-rate-based W08 correction. A similar result holds true for the IK09 correction (not shown). Thus application of a correction to XBT fall-rate equations (at least for the two discussed in this paper) does not completely eliminate the upper ocean XBT warm bias. In particular W08 results clearly document [*Wijffels et al.*, 2008, Figure 9] that the regression technique they use to compute their fall-rate correction equation produces errors. Although this uncorrected bias in the upper 100 m of the water column does not contribute to a substantial error in the OHC700 global integral, systematic errors of order 0.1–0.2°C in the upper 100 m of the ocean may be of importance for properly

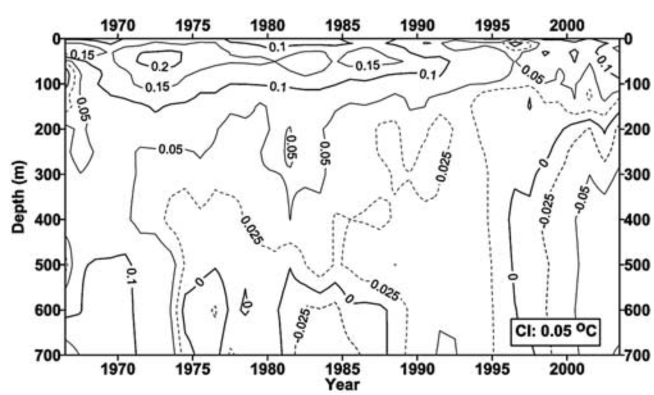

Figure 3. Time series of the offsets (°C) between XBT and OSD/CTD data after the *Wijffels et al.* [2008] bias corrections have been applied based on the median of the offsets. Calculations are based on at least 30 overlapping $2° \times 4°$ boxes per year and level.

estimating tropical cyclone heat potential or for other purposes.

[16] It would be preferable to correct each individual XBT based on its probe type because different XBT probe types have different fall-rates. However there is a lack of metadata for many XBT profiles that would allow us to do this without reducing the amount of data available for computations. IK09 assumed a single fall-rate equation for all unknown XBT types. The agreement shown in Figure S9 suggests that this may not be a bad assumption for the computation of the global integral of OHC700.

4. Global and Basin Times Series

[17] Figure S11 shows time series of OHC700 for individual ocean basins as well as the world ocean. Both the Pacific and Atlantic oceans show decreases after 2005–06 whereas the Indian Ocean does not. The linear trend accounts for 89 and 85% of the variance in the Atlantic and world ocean respectively and 68 and 52% in the Pacific and Indian oceans respectively for the 1969–2008 period.

5. Global Seasonal OHC Estimates

[18] We are beginning an effort to compute seasonal and eventually monthly OHC estimates and make these diagnostic quantities available within a few months after each observation period ends. Towards this effort we have computed seasonal OHC700 estimates for 1955–2008 which are shown in Figure S12. The individual time series are similar which means that our estimates are relatively stable even with the relative lack of data in parts of the world ocean. However this is not equivalent to stating that we have enough data to capture all the variability that could contribute to these integrals if we had a more comprehensive database. We use these seasonal estimates to compute confidence intervals for our yearly time series and these are shown in Figure S13. Two yearly ocean OHC700 estimates are shown in Figure S13. One is our "all-data" yearly estimate approach [*Levitus et al.*, 2000, 2005a] and the other is the average of our four seasonal estimates. The curves are generally close. Differences between the curves in an individual year can be due to sampling bias differences between seasons in these years and actual seasonal variability. Figure S14 shows our seasonal estimates as one continuous time series plotted with our annual mean (average of four seasons) time series.

6. Discussion

[19] Correcting for XBT biases reduces the magnitude of the interdecadal variability of our earlier estimates of OHC700 but has relatively little effect on our previous [*Levitus et al.*, 2005a] estimate of the long-term OHC trend. It is important to note that as additional data becomes available that our results may change somewhat because of better data coverage and more difference pairs becoming available for correcting instrumental biases. To the extent that the XBT temperature bias is due to fall-rate inaccuracies our method of correcting temperature values empirically from comparison with near-contemporaneous OSD/CTD data can be criticized. This is because for a purely fall-rate induced temperature bias, the temperature error for any particular XBT profile depends on the local stratification. We have shown (Figures S7 and S8) that we have reduced the XBT bias to near zero for the global integral as a function of depth and time but there are certainly local differences due to the local stratification in different regions. The agreement between our OHC700 time series and IK09 which is estimated assuming that the XBT bias is solely due to fall-rate error suggests that our two OHC700 global time series are fairly robust as to the two types of XBT bias correction techniques that were applied. As noted earlier the IK09 does not eliminate the time-varying bias in the upper 100 m of the water column. There is unquestionably more work to be done in understanding and developing corrections for the XBT and MBT biases discussed in this paper.

[20] Because of the importance of OHC as a major component of earth's heat balance it needs to be accurately monitored. Analyses using independent data types such as those provided by *Dickey et al.* [2008] are important in evaluating OHC estimates.

[21] All data used in this study as well as the yearly and seasonal gridded heat content fields are available at http://www.nodc.noaa.gov/OC5/indprod.html.

[22] **Acknowledgments.** This work was supported by the NOAA/DOE Climate Change Data and Detection Program and the NOAA Office of Climate Observation Program. We thank the many scientists, technicians, data center staff, and data managers for their contributions of data to the IOC/IODE and ICSU/World Data Center systems which has allowed us to compile the database used in this work. The float data were collected and made freely available by the International Argo Project (a pilot program of the Global Ocean Observing System) and contributing national programs and are available at http://www.argo.net. We thank V. Gouretski, C. Domingues, M. Ishii and their colleagues for making their results available to us. We thank our colleagues at the Ocean Climate Laboratory for their work in constructing the *World Ocean Database*. Thanks to Ken Casey and Charles Sun of NODC for reviewing the manuscript of this paper. The views, opinions, and findings contained in this report are those of the authors, and should not be construed as an official NOAA or U.S. Government position, policy, or decision.

References

Barnett, T. P., D. W. Pierce, and R. Schnur (2001), Detection of anthropogenic climate change in the world's oceans, *Science*, *292*, 270–273.

Barnett, T. P., D. W. Pierce, K. M. AchutaRao, P. J. Gleckler, B. D. Santer, J. M. Gregory, and W. M. Washington (2005), Penetration of human-induced warming into the world's oceans, *Science*, *309*, 284–287.

Boyer, T. P., J. I. Antonov, O. K. Baranova, H. Garcia, D. R. Johnson, R. A. Locarnini, A. V. Mishonov, M. T. Pitcher, and I. Smolyar (2006), *World Ocean Database 2005, Introduction, NOAA Atlas NESDIS*, vol. 60, edited by S. Levitus, 190 pp., NOAA, Silver Spring, Md.

Dickey, J. O., S. L. Marcus, and J. K. Willis (2008), Ocean cooling: Constraints from changes in Earth's dynamic oblateness (J_2) and altimetry, *Geophys. Res. Lett.*, *35*, L18608, doi:10.1029/2008GL035115.

Domingues, C. M., J. A. Church, N. J. White, P. J. Gleckler, S. E. Wijffels, P. M. Barker, and J. R. Dunn (2008), Improved estimates of upper-ocean warming and multi-decadal sea-level rise, *Nature*, *453*, 1090–1095.

Gouretski, V., and K. P. Koltermann (2007), How much is the ocean really warming?, *Geophys. Res. Lett.*, *34*, L01610, doi:10.1029/2006GL027834.

Ishii, M., and M. Kimoto (2009), Reevaluation of historical ocean heat content variations with time-varying XBT and MBT depth bias corrections, *J. Oceanogr.*, in press.

Levitus, S., J. Antonov, T. P. Boyer, and C. Stephens (2000), Warming of the world ocean, *Science*, *287*, 2225–2229.

Levitus, S., J. L. Antonov, J. Wang, T. L. Delworth, K. W. Dixon, and A. J. Broccoli (2001), Anthropogenic warming of Earth's climate system, *Science*, *292*, 267–270.

Levitus, S., J. Antonov, and T. Boyer (2005a), Warming of the world ocean, 1955–2003, *Geophys. Res. Lett.*, *32*, L02604, doi:10.1029/2004GL021592.

Levitus, S., S. Sato, C. Maillard, N. Mikhailov, P. Caldwell, and H. Dooley (2005b), Building ocean profile-plankton databases for climate and ecosystem research, *NOAA Tech. Rep. NESDIS 117*, 29 pp., NOAA, Silver Spring, Md.

Locarnini, R. A., A. V. Mishonov, J. I. Antonov, T. P. Boyer, and H. E. Garcia (2006), *World Ocean Atlas 2005*, vol. 1, *Temperature, NOAA Atlas NESDIS*, vol. 61, edited by S. Levitus, 182 pp., NOAA, Silver Spring, Md.

Wijffels, S. E., J. Willis, C. M. Domingues, P. Barker, N. J. White, A. Gronell, K. Ridgway, and J. A. Church (2008), Changing expendable bathythermograph fall rates and their impact on estimates of thermosteric sea level rise, *J. Clim.*, *21*, 5657–5672.

J. I. Antonov, T. P. Boyer, H. E. Garcia, S. Levitus, R. A. Locarnini and A. V. Mishonov, National Oceanographic Data Center, NOAA, 1315 East West Highway, Room 4326, Silver Spring, MD 20910-3282, USA. (sydney.levitus@noaa.gov)

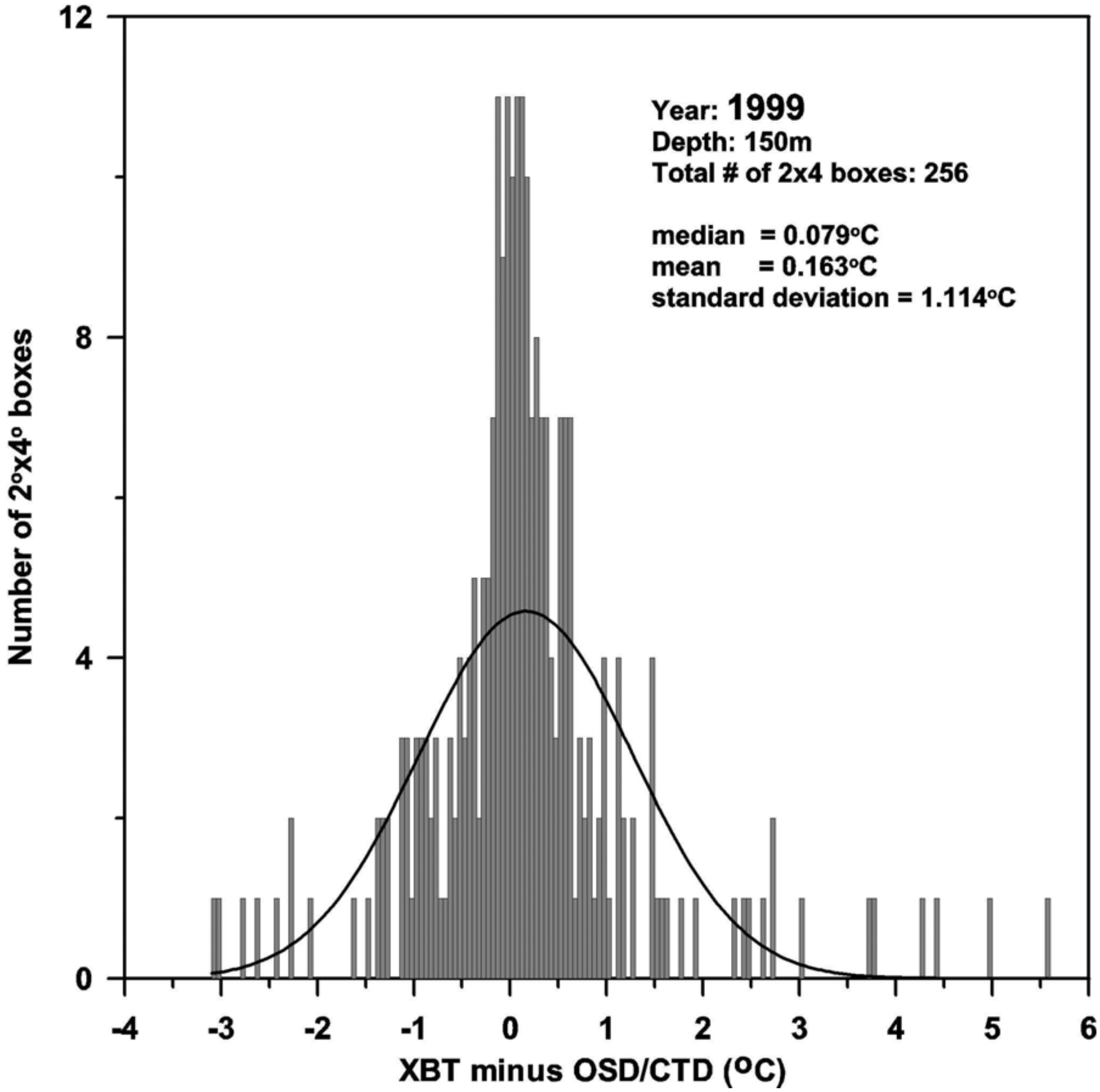

Figure S1 Frequency distribution of 2° x 4° XBT minus OSD/CTD temperature differences (°C) for 1999 at 150 m depth.

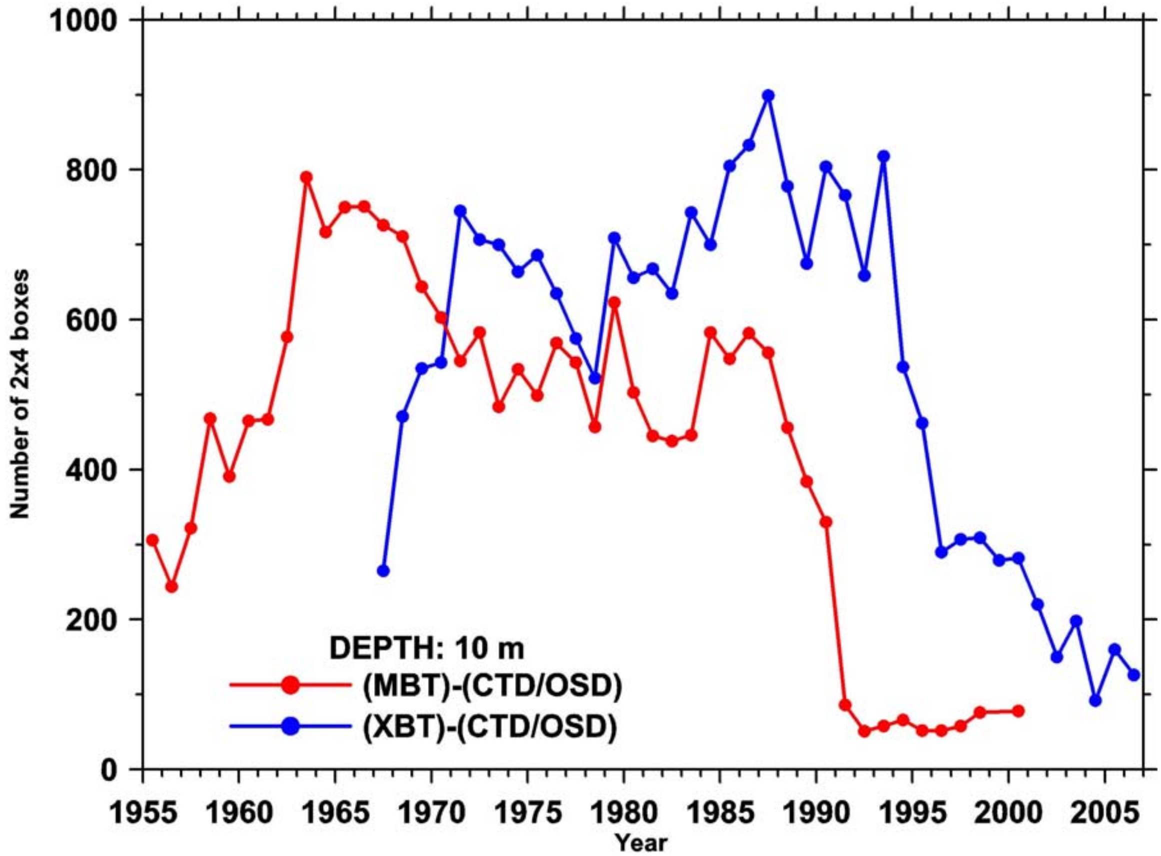

Figure S2. Time series of the number of 2° x 4° boxes per year of the MBT minus OSD/CTD difference pairs and a similar series for XBT minus OSD/CTD difference pairs.

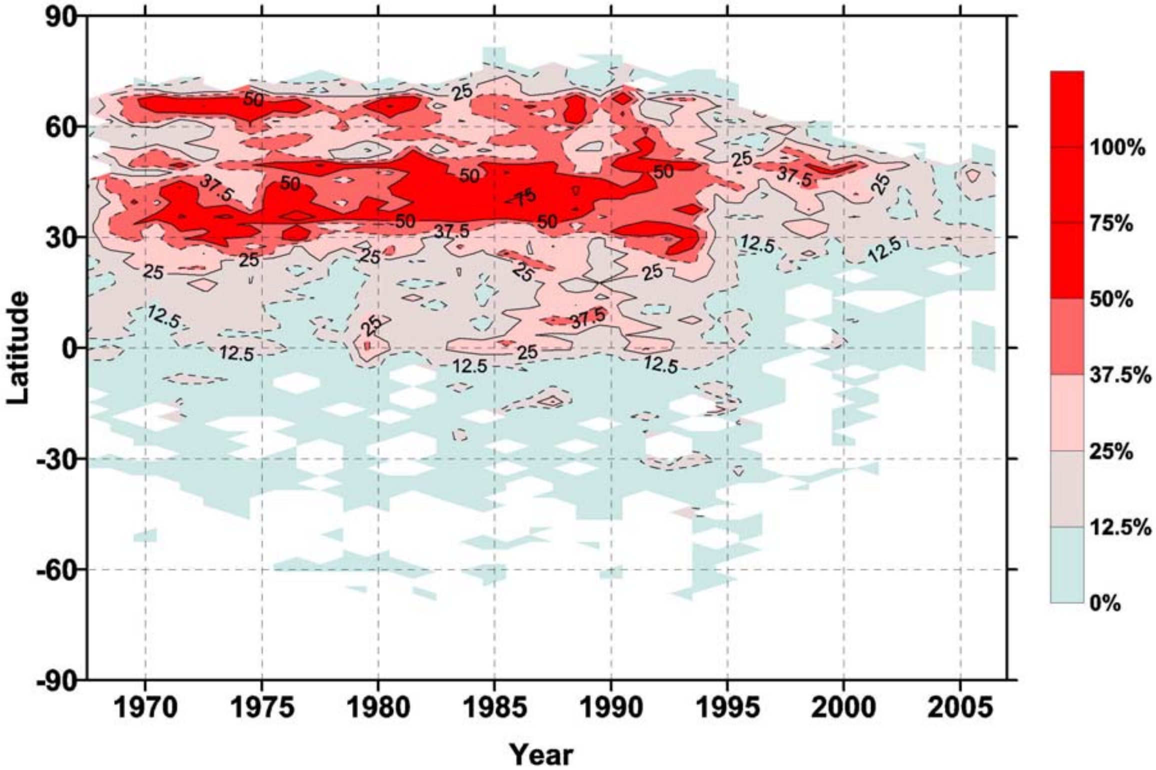

Figure S3. Percent ocean area of 2-degree latitude belts with 2° latitude x 4° longitude boxes containing XBT – (OSD/CTD) differences.

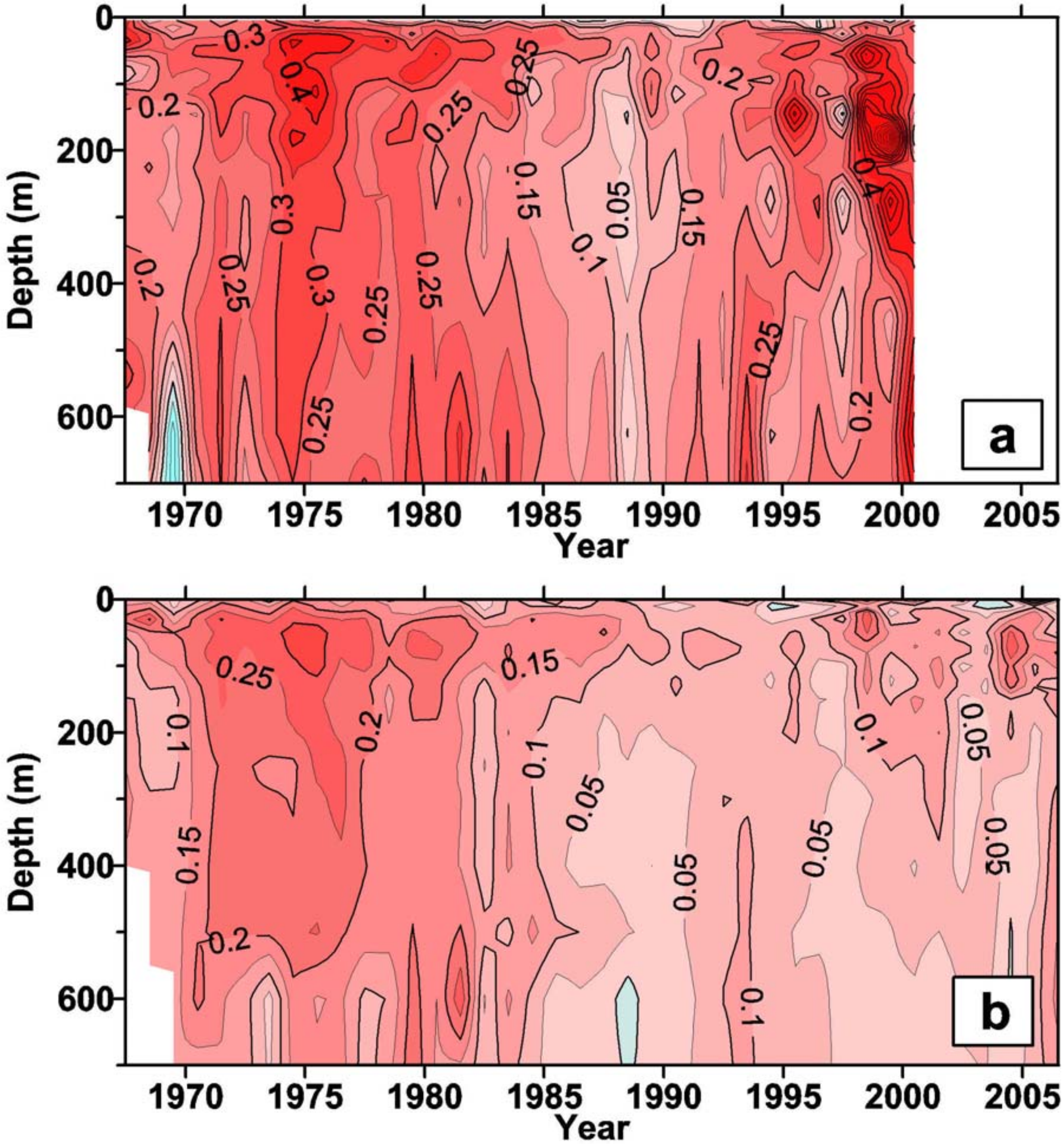

Figure S4. (a) Time series of the offsets based on arithmetic mean of the offsets (°C) between XBT and OSD/CTD data from *Gouretski and Koltermann* [2007]. (b) Time series of the offsets based on median of the offsets (°C) between XBT and OSD/CTD data for this study. Calculations are based on at least 30 overlapping 2° x 4° boxes per year and level. Red indicates positive value, blue indicates negative values.

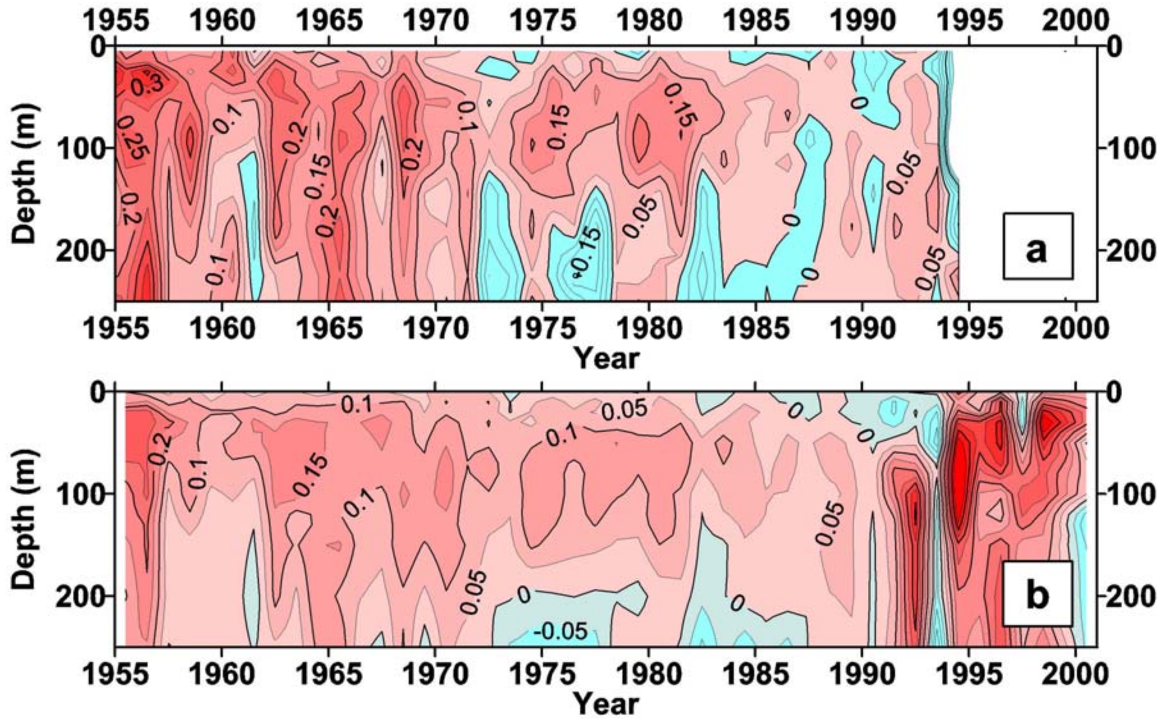

Figure S5. (a)Time series of offsets based on arithmetic mean of the offsets (°C) between MBT and OSD/CTD data from *Gouretski and Koltermann* [2007]. (b) Time series of offsets based on the median of the offsets (°C) between MBT and OSD/CTD for this study. Calculations are based on at least 30 overlapping 2° x 4° boxes per year and level. Red indicates positive value, blue indicates negative values.

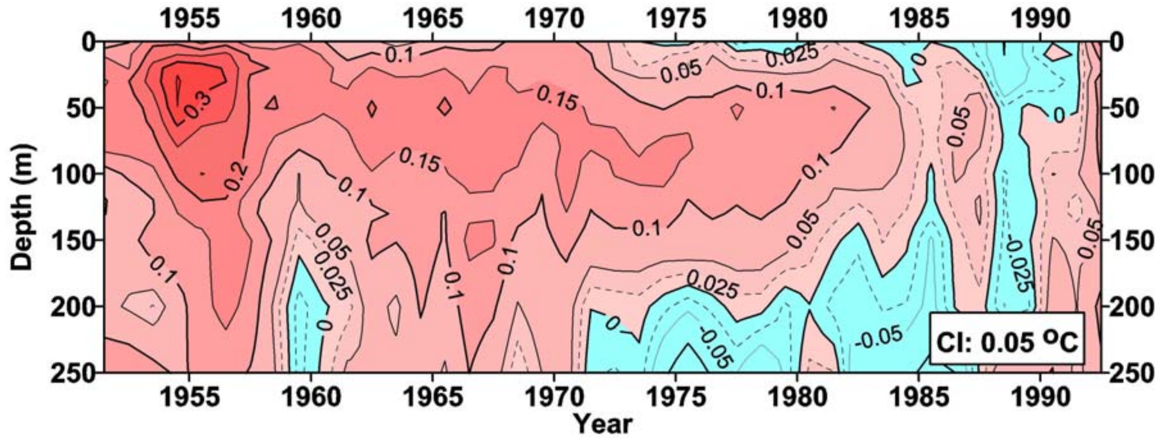

Figure S6. Time series (5-year running means) of the temperature corrections based on medians of the differences (°C) applied to MBT observations. Calculations are based on at least 30 overlapping 2°x4° boxes per year and level.

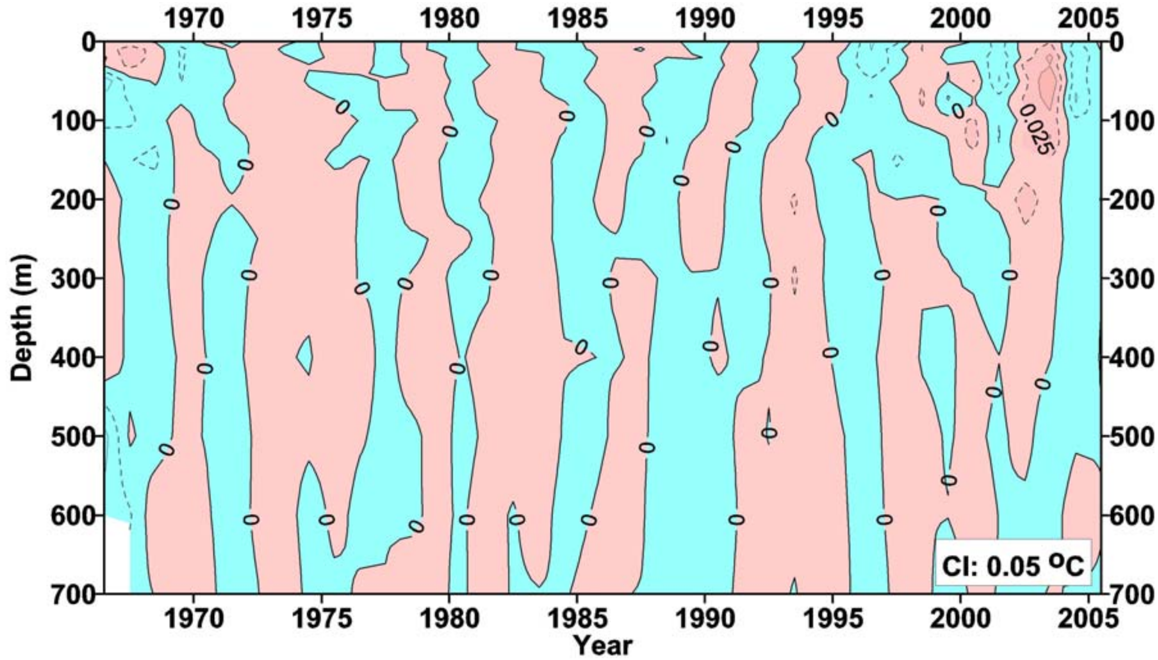

Figure S7. Time series of the offsets (°C) between XBT and OSD/CTD based on the median of the offsets after bias corrections have been applied twice. Calculations are based on at least 30 overlapping 2° x 4° boxes per year and level. Red indicates positive value, blue indicates negative values.

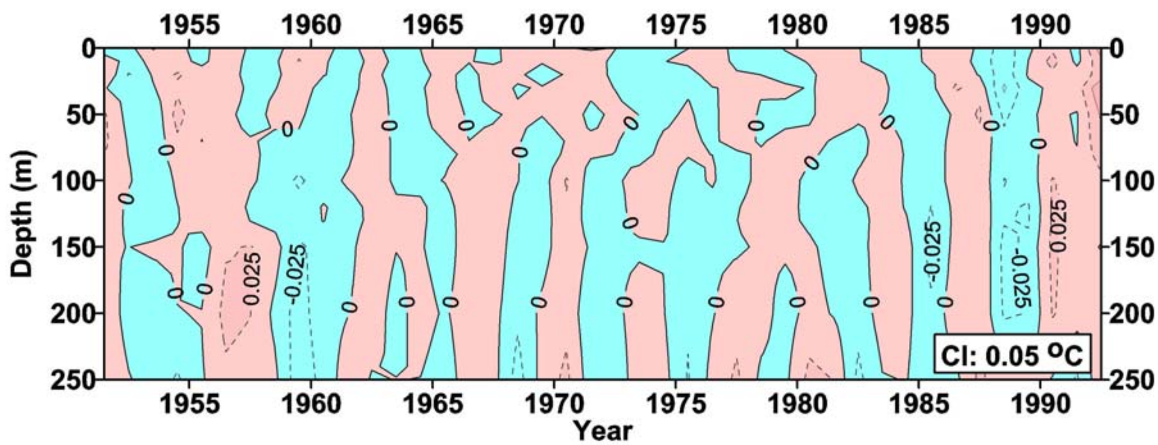

Figure S8. Time series of the offsets (°C) between MBT and OSD/CTD after bias corrections have been applied twice based on the median of the offsets. Calculations are based on at least 30 overlapping 2° x 4° boxes per year and level. Red indicates positive value, blue indicates negative values.

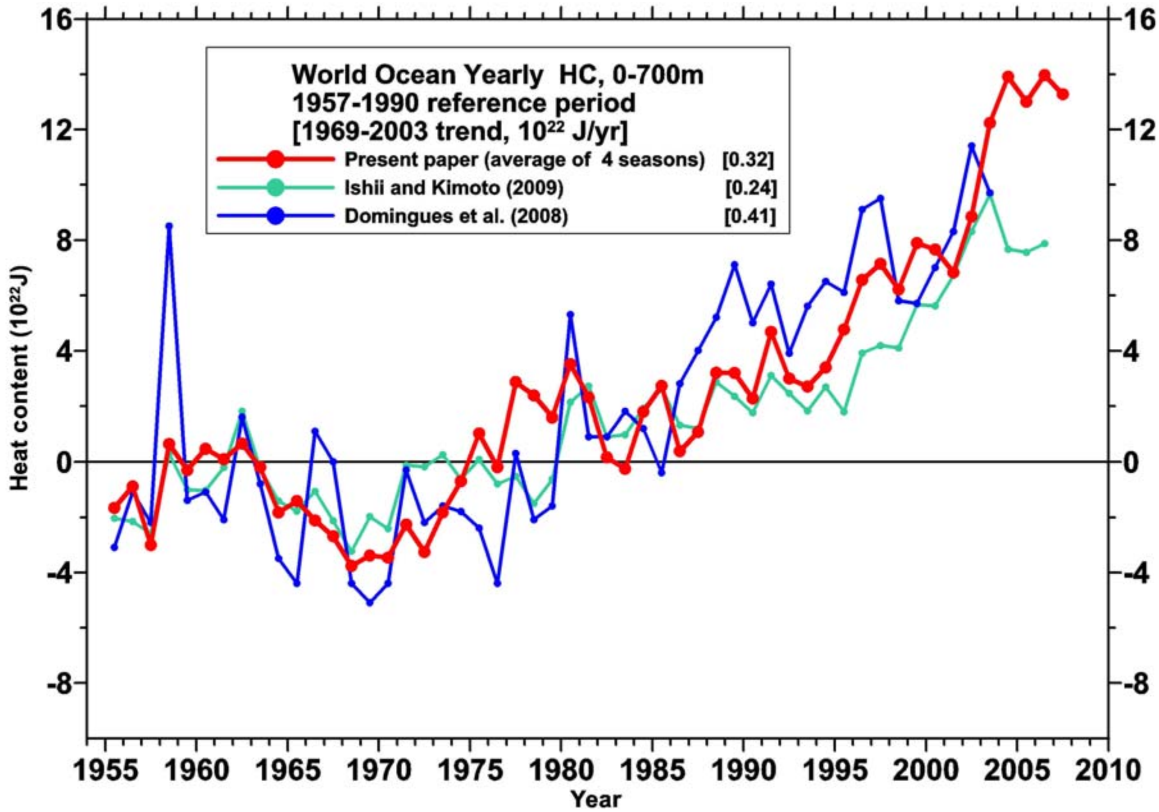

Figure S9. Yearly time series of ocean heat content (10E+22 J) for the 0-700 m layer from this study and from *Domingues et al.* [2008] and Ishii and Kimoto [2008]. Linear trends for each series for 1969-2008 given in the upper left portion of the figure. Reference period is 1957-1990.

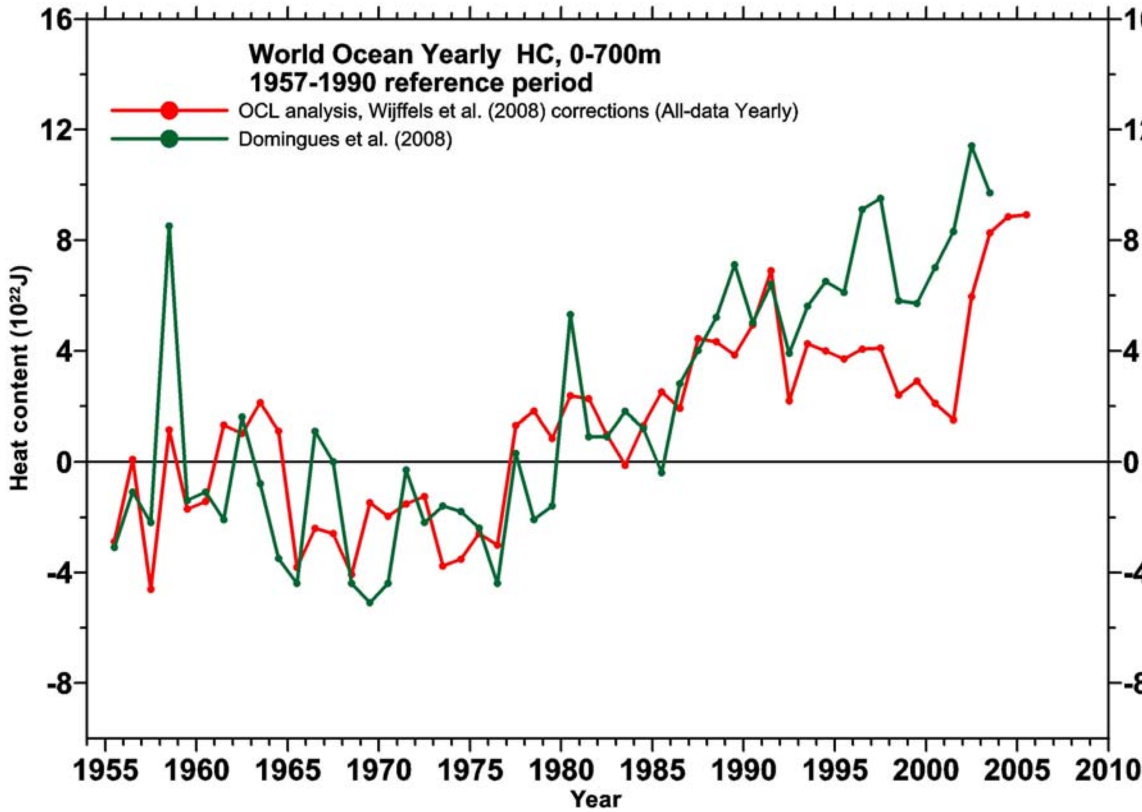

Figure S10. Yearly time series of ocean heat content (10E+22 J) for the 0-700 m layer from *Domingues et al.* [2008] and based on application of the Wijffels et al. [2008) XBT bias correction to our profile database. Linear trends for each series for 1969-2007 given in the upper left portion of the figure. Reference period is 1957-1990.

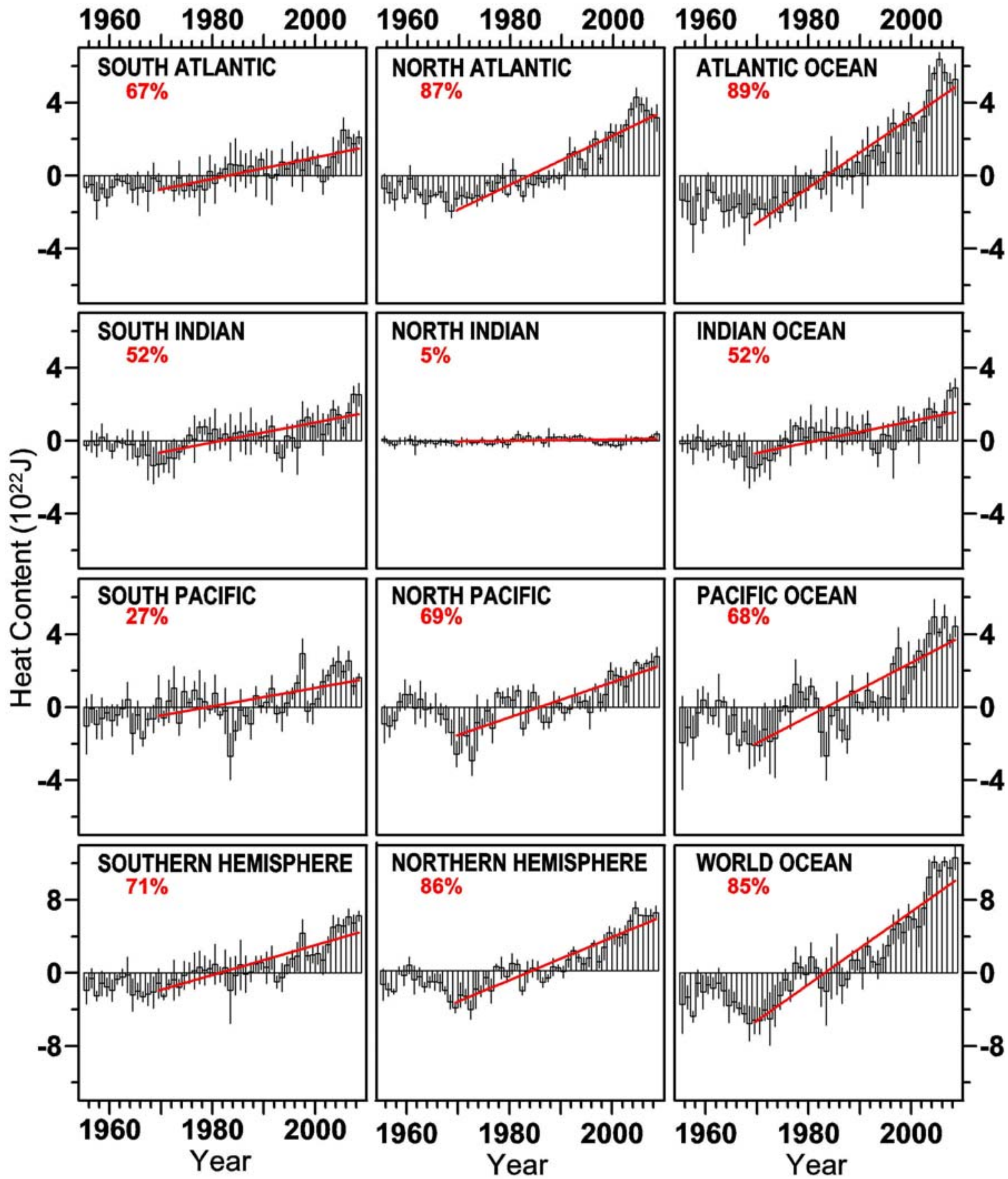

Figure S11. Time series (1955-2008) of yearly ocean heat content (1022J) for the 0-700 m layer of the world ocean and individual ocean basins. The linear trend is shown in each panel for 1969-2007. The percentage in the upper left of each panel each panel is the percent variance accounted for by the linear trend. The vertical lines centered on each yearly estimate represent +/- 2*S.E. determined from the four individual seasonal estimates of heat content for each year plotted. Reference period is 1955-2006.

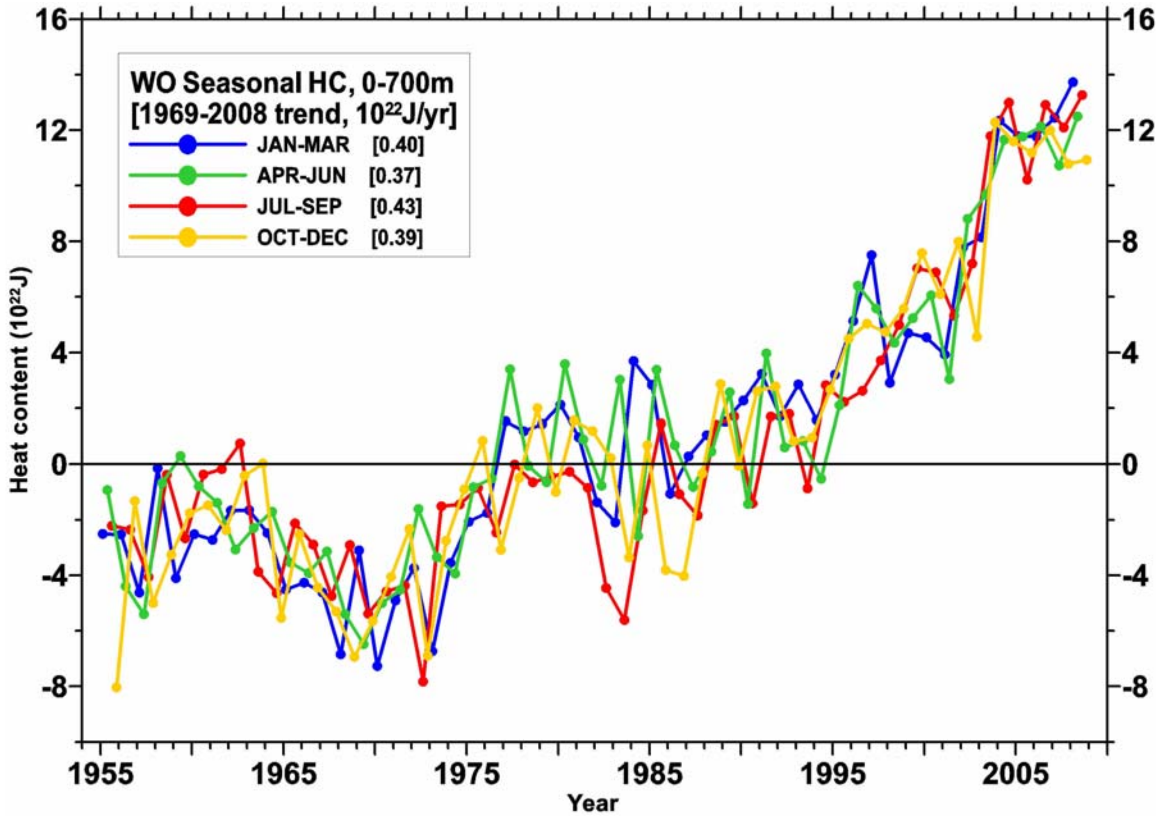

Figure S12. Seasonal time series of yearly ocean heat content (10E+22 J) for the 0-700 m from this study and their trends for 1955-2008. Linear trends for each season for 1969-2008. Reference period is 1955-2006.

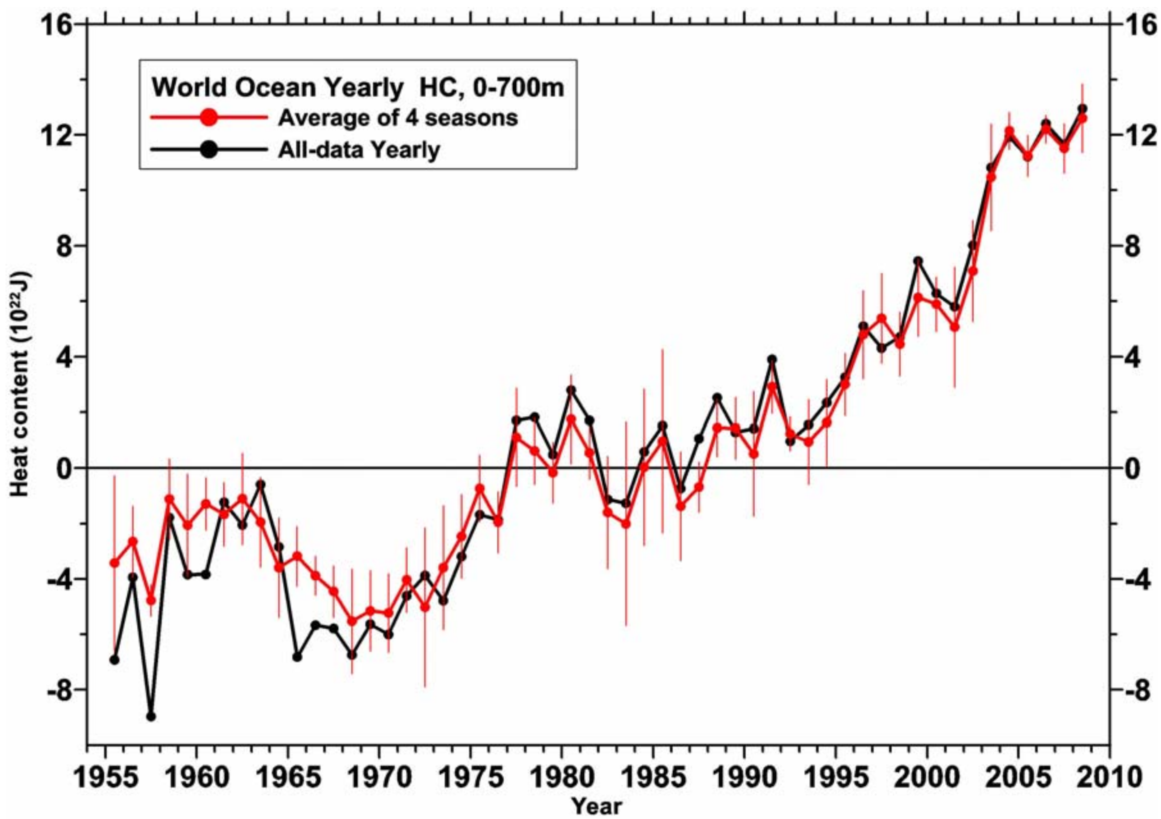

Figure S13. Yearly time series of ocean heat content (10E+22 J) for the 0-700 m layer based on the all-data yearly fields and the average of the four seasonal yearly fields. Plotted about the average of the four seasonal yearly series is +/- 2*S.E. of the mean for each year based on the four seasonal values.

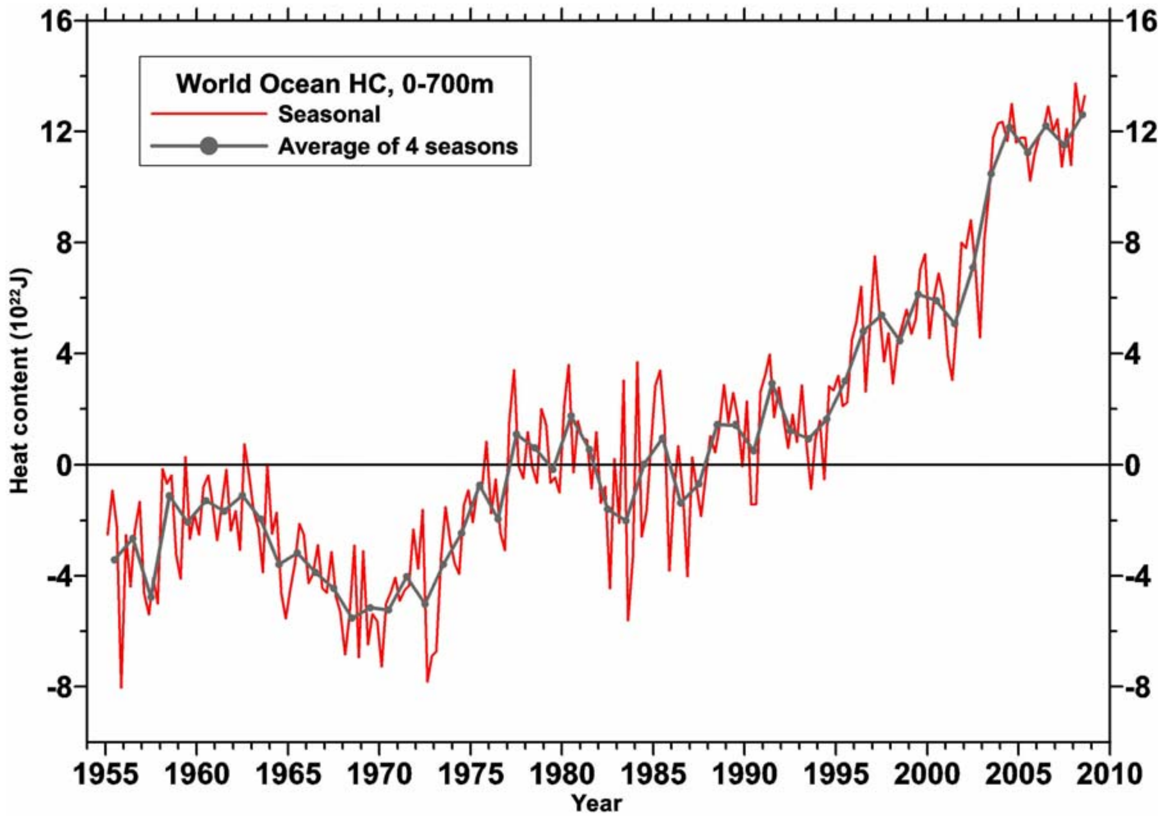

Figure S14. Time series of seasonal OHC700 (10E+22 J) estimates and annual mean of the four seasons.

Table T1. Change in ocean heat content and mean temperature for the 0-700 m layer for the world ocean and individual basins as determined by the linear trend for the 1969-2008 period. Heat storage is per unit area of ocean surface.

OceanBasin	HTrend	HStorage	HChange	TChange
World_Ocean	0.398	0.364	15.913	0.168
N_Hemisphere	0.235	0.521	9.392	0.248
S_Hemisphere	0.163	0.254	6.522	0.115
Atlantic	0.193	0.626	7.721	0.301
North_Atlantic	0.135	0.813	5.390	0.409
South_Atlantic	0.058	0.409	2.330	0.187
Pacific	0.147	0.265	5.873	0.121
North_Pacific	0.097	0.387	3.861	0.178
South_Pacific	0.050	0.165	2.012	0.075
Indian	0.058	0.253	2.317	0.114
North_Indian	0.003	0.101	0.138	0.047
South_Indian	0.055	0.279	2.180	0.125

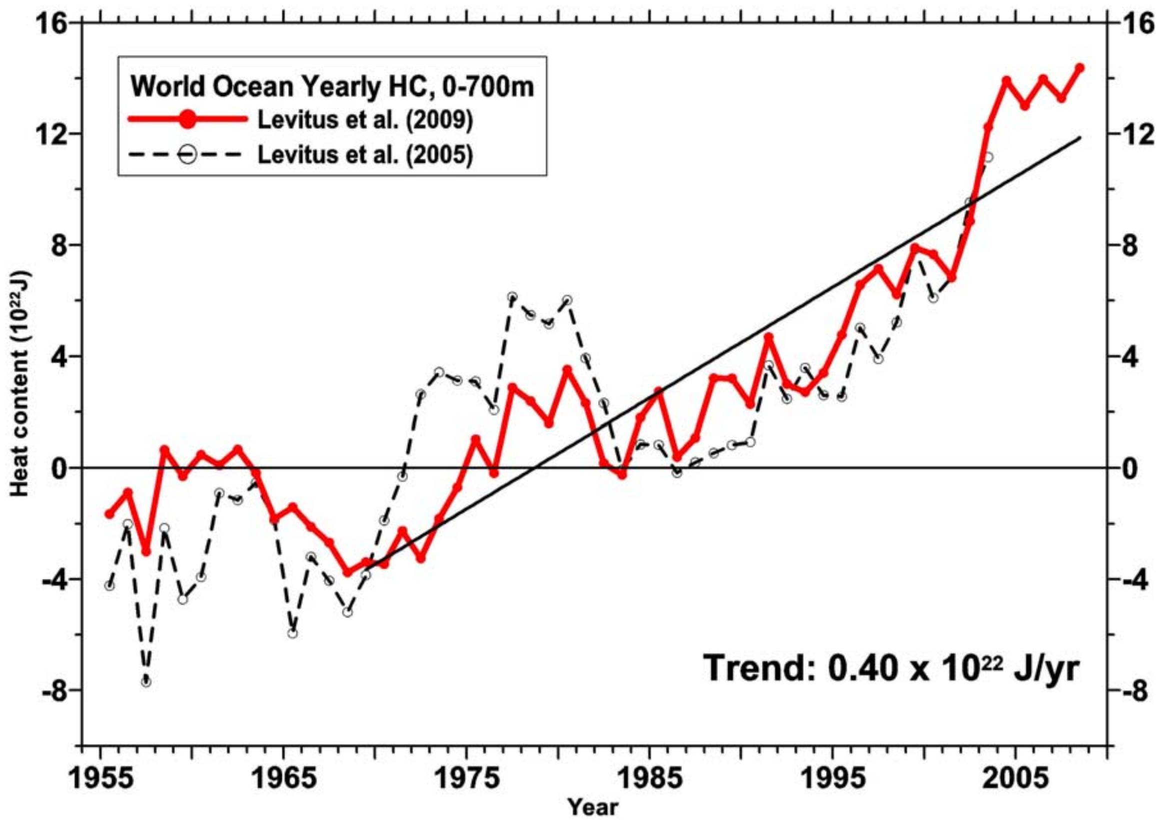

Figure 1. Time series of yearly ocean heat content (10^{22}J) for the 0-700 m layer from this study (solid) and from *Levitus et al.* [2005a] (dashed). Each yearly estimate is plotted at the midpoint of the year. Reference period is 1957-1990.

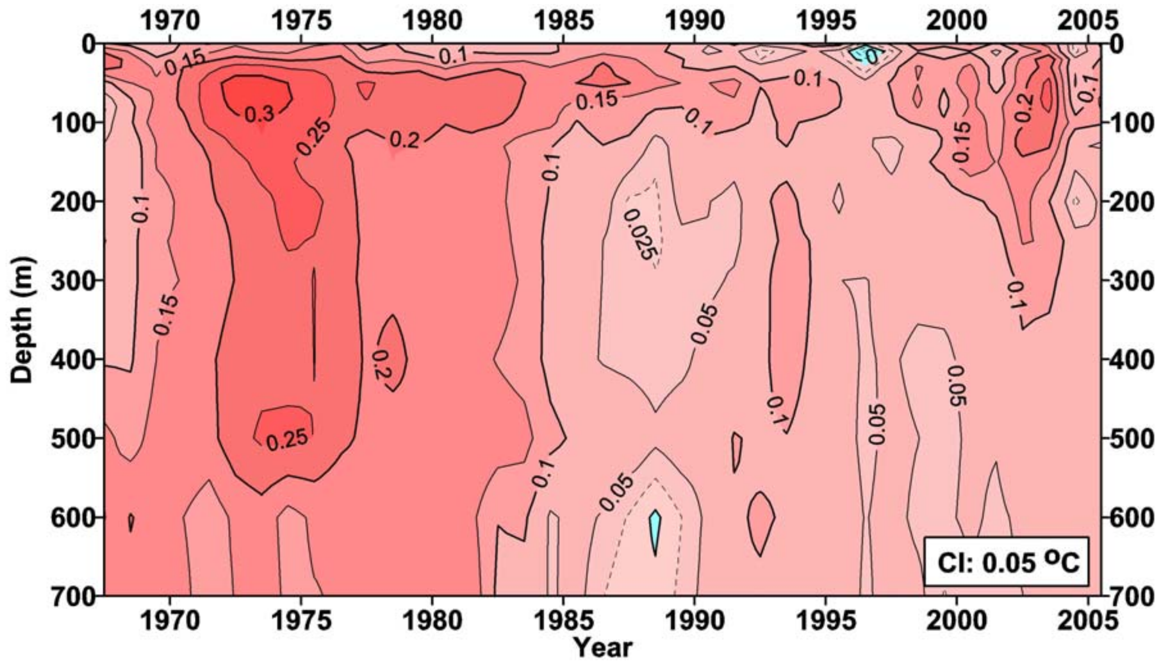

Figure 2. Time series (5-year running means) of the temperature corrections based on medians of the differences (°C) applied to XBT observations. Calculations are based on at least 30 overlapping 2°x4° boxes per year and level.

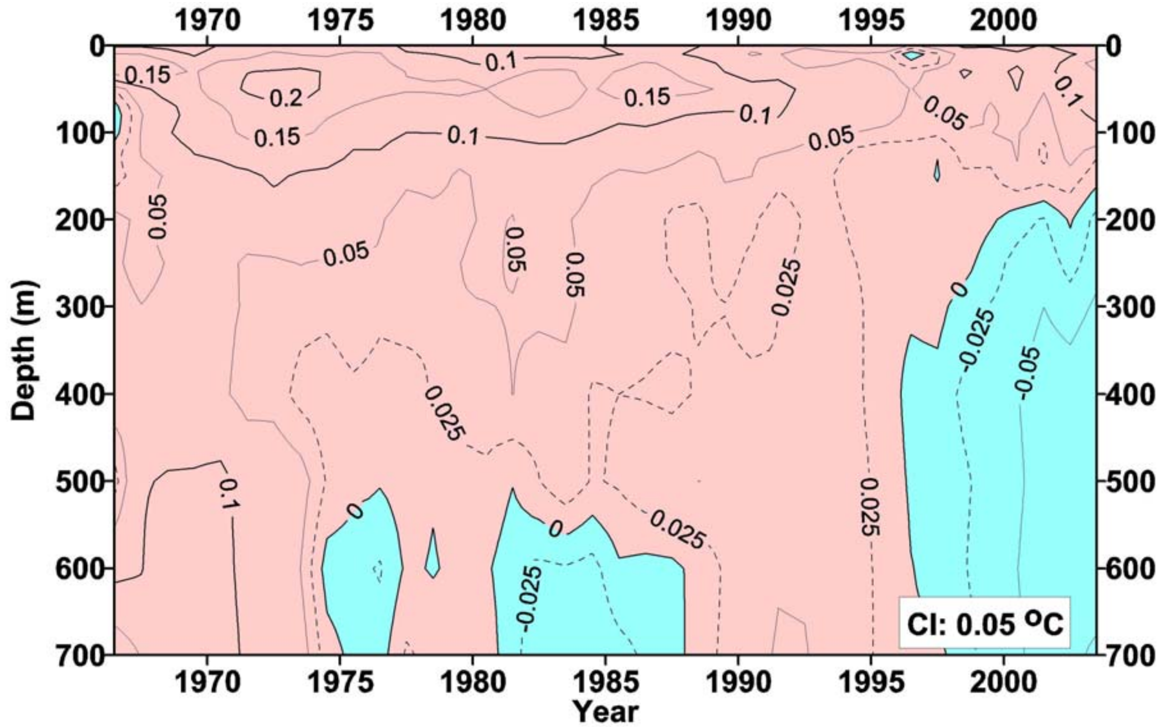

Figure 3. Time series of the offsets (°C) between XBT and OSD/CTD data after the *Wijffels et al.* [2008] bias corrections have been applied based on the median of the offsets. Calculations are based on at least 30 overlapping 2° x 4° boxes per year and level. Red indicates positive values, blue indicates negative values.